Water Air Soil Pollut (2015) 226: 14
DOI 10.1007/s11270-014-2224-2

Effect of Humic Acid on Arsenic Adsorption and Pore Blockage on Iron-Based Adsorbent

Hoda Fakour · Yi-Fong Pan · Tsair-Fuh Lin

Received: 5 March 2014 / Accepted: 10 November 2014 / Published online: 4 February 2015

Abstract The effect of humic acid (HA), on the adsorption and transport of arsenic (As) onto and within a model iron oxide-based adsorbent, iron oxide-coated diatomite (IOCD), is investigated. Experimental results indicate that the adsorption of both As and HA is highly pH-dependent. As uptake was suppressed by HA, with the level of suppression increasing with HA concentration. The suppression is attributed to the partial coverage of the adsorption sites, as confirmed by elemental analysis. Adsorption energy analysis indicates that for As(III), the main interaction with IOCD is physical adsorption, whereas for As(V), it is more likely ion exchange. The presence of HA may alter the adsorption energy and interaction of As with the adsorbent, particularly at higher HA concentrations. Kinetic results indicate that HA did not affect the diffusional transport of As in systems with both As and HA. However, for IOCD preloaded with HA, the adsorption kinetics of As was significantly slower, although the As uptake was similar to the conditions of co-sorption with HA. The slower kinetics and similar equilibrium uptake of As in the HA-preloaded IOCD system may be attributed to the partial blockage of the intraparticular pores within IOCD, which slowed down the diffusion of As.

Keywords Adsorption · Arsenic · Diatomite · Iron oxide · Natural organic matter

H. Fakour · Y.-F. Pan · T.-F. Lin (✉)
Department of Environmental Engineering, National Cheng Kung University,
Tainan City, Taiwan
e-mail: tflin@mail.ncku.edu.tw

H. Fakour
e-mail: p58997034@mail.ncku.edu.tw

H. Fakour
e-mail: fakour.h@gmail.com

Y.-F. Pan
e-mail: p5895103@mail.ncku.edu.tw

1 Introduction

Arsenic (As) in groundwater has become a worldwide concern due to its wide distribution and severe threat to human health (Guo et al. 2012). The occurrence and behavior of As in the environment have been extensively reviewed (Cullen and Reimer 1989; Tamaki and Frankenberger 1992; Matschullat 2000; Mandal and Suzuki 2002; Smedley and Kinniburgh 2002). As may cause skin lesions and cancers as a result of its preferential reaction with sulfhydryl groups in enzymes (Yoshida et al. 2004; Bahar et al. 2013). Hence, the World Health Organization (WHO), the US Environmental Protection Agency (USEPA), and Taiwan Environmental Protection Administration (TWEPA) set the drinking water

guideline value and standard to 10 μg/L (USEPA 2001; TWEPA 2014).

In natural groundwater, inorganic As mainly presents in arsenite (As(III)) and arsenate (As(V)). The predominant species of As(V) are $H_2AsO_4^-$ (pH=2–6.5) and $HAsO_4^{2-}$ (pH=6.5–11.5), whereas As(III) is present as a neutral molecule from (H_3AsO_3) at pH lower than 9.2 (Bard et al. 1985). Several methods have been developed for As removal from water, including coagulation, adsorption and ion exchange, and membrane separation (USEPA 1999; Liu et al. 2012). Among the common treatment methods, adsorption onto metal oxides is one of the promising methods appropriate in both small- and large-scale applications (Lin et al. 2006; Simsek et al. 2013).

The adsorption of As is known to be adversely affected by the water matrix, including pH and competing ions such as carbonate, sulfate, phosphate, silicate, and natural organic matter (NOM) (Guan et al. 2009). NOM molecules have unique combinations of functional groups, including carboxylic, esteric, phenolic, quinone, amino, nitroso, sulfhydryl, hydroxyl, and other moieties, the majority of which are negatively charged at neutral pH (Liu et al. 2013). In natural waters, NOM is typically found at concentrations between 1 and 50 mg/L (Redman et al. 2002) and may compete with target pollutants for adsorption onto solid surfaces by reducing their adsorption rates and equilibrium capacities (Summers et al. 1989). Accordingly, influences of NOM on As sorption and speciation are expected to be great (Kalbitz and Wennrich 1998; Redman et al. 2002; Anawar et al. 2003). NOM may bind directly to an oxide surface, and if similar sites are employed in As adsorption, this may interfere with the As adsorption process (Redman et al. 2002; Lv et al. 2013). One of the most abundant natural organic substances on the earth's surface is humic acid (HA) (Yu 2001; Loffredo and Senesi 2006). HA is a kind of multi-phenolic large molecular weight which is very active chemically (Fox 1983; Murphy et al. 1992; Jansen et al. 1996; Yu 2001).

Among different adsorbent media, iron oxides, oxyhydroxides, and hydroxides, including amorphous hydrous ferric oxide (FeO-OH), goethite (−FeO-OH), and hematite (−Fe_2O_3), are promising adsorbents for removing both As(III) and As(V) from water (Sun and Doner 1998; Dixit and Hering 2003; Jang et al. 2008). It is noted that most iron oxides are present as fine powders that are difficult to separate from solution after adsorption has reached equilibrium (Lai et al. 2000). To overcome this problem, many solids coated with iron oxides have been employed instead. Typical substrates used in the processes include zeolite (Jeon et al. 2009; Jiménez-Cedillo et al. 2009), montmorillonite (Ramesh et al. 2007), cement (Kundu and Gupta 2006), activated carbon (Mondal et al. 2007), and sand (Benjamin et al. 1996; Lai et al. 2000). Although application of iron oxide-coated porous solid has been studied for As removal (Redman et al. 2002; Dhiman and Chaudhuri 2007; Hristovski et al. 2009), little information is available on the adsorption of As species using diatomite coated with iron oxide (Pan et al. 2010). Raw diatomite ($SiO_2 \cdot nH_2O$) is a soft and lightweight sedimentary rock consisting principally of silica microfossils of aquatic unicellular alga and is available in large deposits around the world (Pan et al. 2010). Diatomite is a natural material that can be used as a substrate for iron oxide coating. In our previous work, a novel granular adsorbent, iron oxide-coated diatomite (IOCD), was developed and evaluated for its adsorption of As(V) from water (Pan et al. 2010). According to results, the adsorption capacity of As(V) on an iron-coated product is relatively high and the kinetics is fast. Although IOCD showed high efficiency in As treatment, there is still a lack of detailed information regarding the specific effect of coexisting compounds such as humic substances on As adsorption. Taking possible effects of humic substances on fate and transport of toxic compounds into account, a systematic study is needed to quantify the influence of NOM on As adsorption onto metal oxides in aqueous systems.

In order to attain a better understanding of applying an iron-coated product for As removal in field applications, the present study investigates the effects of HA on As adsorption by IOCD in simulated As(III)- and (V)-contaminated waters. Through batch experiments, the effect of HA on the transport and adsorption of As onto IOCD is evaluated. The data are analyzed to characterize the impact of HA on adsorption capacities and diffusion rates of As onto IOCD.

2 Materials and Methods

2.1 Materials

Iron-coated product was prepared using a method described by Pan et al. (2010). Iron oxide coated on the surface of IOCD was α-Fe_2O_3 (hematite). The IOCD, coated with iron oxide for two times and with mean particle size of 0.11 mm, was employed in this study due to its high efficiency in As removal based on earlier results (Pan et al. 2010).

$Na_2HAsO_4{\cdot}7H_2O$ (98 % in purity, Alfa Aesar, UK) and $NaAsO_2$ (GR grade, Sigma, USA) were used as sources of As(V) and As(III) stock solutions (50 mg/L), respectively, to prepare experimental solutions of specified concentrations. Commercial HA (technical grade) was obtained from Aldrich Chemical and dissolved into ultrapure water (>18.1 MX cm) followed by filtering through 0.45-μm acetate cellulose membranes (Advantec, Japan) for preparing the HA stock solution (1,000 mg/L). HA stock solution was kept in a glass bottle in darkness at 4 °C. All adsorption experiments were performed within 4 weeks after the stock solution was prepared. The pH of the samples was adjusted using 1 M HNO_3 or NaOH, and the expected pH value was maintained until the end of experiments.

2.2 Adsorption Experiments

Experiments on the equilibrium and kinetics of adsorption of As(III) and As(V) with and without HA on IOCD were conducted using 0.1- and 2-L polyethylene bottles, respectively. In each experiment, about 0.2 g/L of adsorbent was added into the bottle. The bottles were then placed on a 360° rotator (TCLP-601P, Taiwan) with a rotation speed of 27±1 rpm at room temperature (25± 3.0 °C). Samples were periodically taken, followed by filtration through a 0.45 μm membrane. Preliminary experiments indicated that the equilibrium of adsorption can be established within 144 h (Pan et al. 2010), which is used for the time of equilibrium experiment.

Equilibrium experiments were conducted to determine the sorption behavior of As(III) and As(V) to the iron-coated product at pH 7.5 (to simulate pH of natural water systems) and different concentrations of HA (5–30 mg/L). All the equilibrium experiments were conducted in duplicate and average values are reported. For kinetic experiments, samples were taken at different time periods before reaching equilibrium and were analyzed for the residual As concentrations in the solutions.

The adsorption uptake, q (mg/g), at any given time was calculated using Eq. (1):

$$q = \frac{(C_0 - C)V}{w} \tag{1}$$

where C_0 is the initial As concentration in the solution (mg/L), C is the residual As concentration (mg/L) at any given time, V is the volume of solution (L), and w is the mass of the adsorbent (g).

A clear understanding of adsorption kinetics of As within the adsorbent will ensure a better prediction of transport behavior of As in the environment. NOM is widespread in the environment and thus may encounter surface sites prior to an influx of As-contaminated water in many cases. Therefore, scenarios with the simultaneous presence of HA and As and/or the introduction of IOCD preloaded with HA into As solutions (pH=7.5) were examined. For the case of simultaneous adsorption, both As (5 mg/L) and HA (5–30 mg/L) were introduced into the system at the same time. For the HA pre-adsorption case, HA (30 mg/L) was first allowed to sorb onto IOCD. After reaching equilibrium (144 h as suggested in preliminary experiments), the solution was filtered through 0.45-μm acetate cellulose membranes to separate IOCD particles. The HA-pre-sorbed IOCD samples were then collected and dried at room temperature overnight. The adsorption kinetics of As was tested by adding the HA-pre-sorbed IOCD to As-containing solution (5 mg/L) to evaluate the effect of HA on As uptake while the sorption sites already occupied. Note that the As concentration chosen is close to many groundwater level in Taiwan, which is near milligrams per liter level (Lin and Wu 2001; Lin et al. 2002).

2.3 Kinetic Models for Adsorption

A pore diffusion model (PDM) was employed to simulate the kinetic data and determine whether HA can affect the diffusion of As species. The PDM, which was modified from that for the vapor transport of volatile organic compounds within activated carbon and soil (Lin et al. 1996; Lin 1997), describes fairly well the As adsorption kinetics within activated alumina (Lin and Wu 2001). The governing equation of the PDM

describing the transport of As species within IOCD particles can be expressed as follows:

$$\varepsilon_P \frac{\partial C_r}{\partial t} + (1-\varepsilon_P)\rho_p \frac{\partial q_r}{\partial t} = \frac{\varepsilon_P}{r^2}\frac{\partial}{\partial r}\left(r^2 D_P \frac{\partial C_r}{\partial r}\right) \quad (2)$$

where ε_p is the porosity (−), C_r is the aqueous concentration within the pore at location r (g/cm^3), t is the time (s), ρ_p is the skeleton density of the IOCD particle (g/cm^3), q_r is the As uptake at location r (g/g), r is the radial coordinate of an IOCD particle (cm), and D_p is the pore diffusivity of As through the intragranular pore space of IOCD (cm^2/s). The appropriate initial and boundary conditions in a batch adsorption system can be expressed as follows:

$$\begin{cases} C_r(0 \le r \le a, t = 0) = 0 \\ \dfrac{\partial C_r}{\partial r}(r = 0, t) = 0 \\ \varepsilon_P D_P|_{r=a} \dfrac{\partial C_r}{\partial r} = k_f\left(C_b - C_{r,s}\right) \end{cases} \quad (3)$$

where k_f is the interphase mass transfer coefficient (cm/s), C_b is the concentration in the bulk aqueous phase (g/cm^3), $C_{r,s}$ is the concentration at the external surface of IOCD, and a is the radius of an IOCD particle (cm). The PDM was coupled with the Langmuir equation to mimic the experimental kinetic curve for As adsorption under a specified condition. In the model, the IOCD particles were considered to be spherical and porous with a constant pore diameter and a uniform distribution of adsorption sites throughout the grain. The As species were assumed to be transported from bulk water to internal surfaces of the IOCD grain by diffusion; the external film diffusion and intragranular pore diffusion were treated as rate-limiting steps. More detailed descriptions of the PDM are available in the literature (Lin and Wu 2001; Pan et al. 2010).

2.4 Equilibrium Isotherm Model

The corresponding adsorption isotherms, plotted as the amount adsorbed by a unit mass of IOCD (q) against the equilibrium concentration of As species in water (Ce), were evaluated with both the Freundlich and Langmuir models. The Langmuir adsorption isotherm is perhaps the most well-known isotherm describing adsorption (Langmuir 1918). The theoretical Langmuir isotherm is often used to describe adsorption of a solute from a liquid solution as follows (Ho et al. 2002):

$$q_e = \frac{q_m K_a C_e}{1 + K_a C_e} \quad (4)$$

where q_e is the equilibrium adsorption capacity (mg/g), q_m is the maximum adsorption capacity (mg/g), K_a is the adsorption equilibrium constant (L/mg), and C_e is the equilibrium liquid phase concentration (mg/L).

The Freundlich isotherm is the earliest known relationship to describe the adsorption isotherm (Freundlich 1906). This fairly satisfactory empirical isotherm can be used for adsorption from diluted solutions. The ordinary adsorption isotherm is expressed as follows:

$$q_e = K_F C_e^{1/n} \quad (5)$$

where K_F is the Freundlich constant and $1/n$ is an empirical constant.

2.5 Analytical Methods

As concentration in solutions was determined using an inductively coupled plasma-optical emission spectrometer (ICP-OES, Ultima 2000) with a detection limit of 5 μg/L. The instrument was calibrated each time before use. During the analysis, each sample was injected three times, and the relative standard deviation (RSD) for the triplicate analysis was within 5 %. Ultraviolet (UV) absorbance at 254 nm (Hitachi UV–VIS spectrophotometer U-2001) was employed for HA measurements as it has been introduced as a parameter to represent the concentration of humic substances (HSs) in water (Najm et al. 1994; Eaton 1995). Given stable absorption characteristics, the UV light absorbance of HSs at a specific wavelength is proportional to their concentration according to Beer's law (Rodrigues et al. 2008). The solution pH was measured using a pH meter (SUNTEX SP-2200), and all batch experiments were run at least in duplicate.

The mineralogy of the model sorbent was characterized using SEM (HITACHI, S-3000N) integrated with energy dispersive X-ray spectroscopy (EDS) (Horiba Emax-Energy) for elemental composition analysis. KaleidaGraph software version 4.0 (USA) was employed for data and curve fittings.

3 Results and Discussion

3.1 Characteristics of the Adsorbent

SEM micrograph and physical properties of the bare diatomite and IOCD-$2_{0.11}$ are given in Fig. 1 and Table 1. As Fig. 1 shows, the high porosity of raw diatomite and well coating with iron oxide made diatomite as a good support medium of iron oxide. More information can be found in Pan et al. (2010).

3.2 Adsorption of As and HA

Figure 2a shows the adsorption of As species onto iron-coated product over a pH range of 2–10. The uptake of arsenate is less than that of arsenite in the pH range of the natural environment. The adsorption behavior of As(V) as a function of pH has been widely reported in the literature (Pierce and Moore 1982; Deschamps et al. 2003; Markovski et al. 2014). Under most pH conditions, As(V) is present in negative ionic form ($H_2AsO_4^-$ at pH=2–6.5 and $HAsO_4^{2-}$ at pH=6.5–11.5) and As(III) is in nonionic form (H_3AsO_3 at pH lower than 9.2). Since the point of zero charge (pHpzc) of hematite is about 8±1 (Zhou et al. 2008), the partial positive charge density of the IOCD surface decreases with increasing solution pH, which consequently decreases the electrostatic attraction between the negatively charged As species and the adsorbent surface, causing a reduction of As(V) uptake (Pan et al. 2010). As also reported by Raven et al. (1998), the lower adsorption of As(V) at high pH values can be attributable to an increased repulsion between the more negatively charged arsenate species and negatively charged surface sites of iron(III) oxide. In addition, the decrease in the adsorption of anionic As species like As(V) on FeOOH has been attributed to an increase in competing hydroxyl anions (OH^-) for adsorption sites with increasing pH (Manna et al. 2003).

Although the toxicity of As(III) is higher than that of As(V), the interaction of As(III) with iron oxides has not received as much attention. Arsenite is generally assumed to be less strongly adsorbed by oxides compared to As(V) (Pierce and Moore 1982; Wilkie and Hering 1996; Nayak et al. 2006). Therefore, in many water treatment practices, As(III) is oxidized first before being treated with adsorption processes (Liu et al. 2012). However, there are some conflicting results regarding the adsorption envelope of As(III) with iron oxide systems. Ferguson and Anderson (1974) observed an increase in As(III) adsorption with increasing pH from 6 to 8, while Raven et al. (1998) showed a trend of increasing adsorption of arsenite with increasing pH, with maximum adsorption at pH 8.2–10. In contrast, Pierce and Moore (1982) and Singh et al. (1988) observed an adsorption maximum at pH 7.0 for iron oxide adsorbents. In the current study, the uptake of As(III) on IOCD increases as pH increases until a pH of about 7 and then decreases as pH increases. The reason is likely due to the fact that the active component in this iron oxide adsorbent for As(III) adsorption is still Fe(III) oxide (Zeng 2004). Hence, the explanations of pH

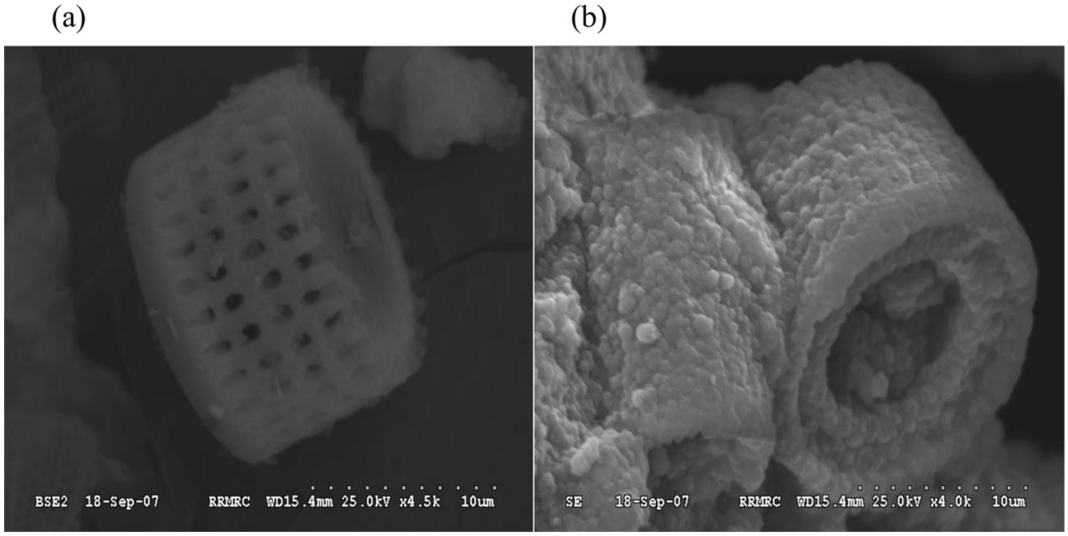

Fig. 1 SEM image of **a** raw diatomite and **b** IOCD-$2_{0.11}$ (Pan et al. 2010)

Table 1 Physical properties and elemental compositions of raw and iron oxide-coated diatomite (Pan et al. 2010)

Property	Raw diatomite	IOCD-$2_{0.11}$[a]
Particle diameter (mm)	0.11±0.008[b]	0.17±0.002[b]
BET surface area (m^2/g)	51	93
Elements (%)[c]		
Oxygen	53.9	29.8
Silica	36.6	6.9
Iron	2.7	62.0

[a] Diatomite (0.11 mm) coated twice with iron oxide

[b] Mean±standard deviation

[c] EDS analysis

effects on As adsorption on Fe(III) oxides can be applied to As(III) system. The adsorption of neutral H_3AsO_3, which is the dominant As(III) species at a wide pH range of 2 to 9, would be less strongly affected by the anion repulsion forces that would likely play an important role in the adsorption of As(V) species at high pH (Biswas and Loeppert 2003). Similar results are reported by Yuan et al. (1987) and Pierce and Moore (1982) for iron oxides suggesting that the best removal efficiency is strongly dependent on careful selection of the relative concentration of As, iron (hydr)oxide, and pH. Overall, Fig. 2a shows that the influence of pH on the adsorption of As(III) and As(V) is different, as the interaction between the two arsenic species and IOCD surface may change differently with pH. This is because an increase in pH reduces the fraction of positively charged surface sites on the IOCD, and since As(V) is in anionic form at most pH conditions, As(V) uptake is thus reduced as the pH increases. For As(III), the uptake does not change significantly as it is mostly in molecular form at pH<9.2 (Lin et al. 2006; Pan et al. 2010).

To investigate the capacity of IOCD for HA adsorption, the adsorption of HA onto the iron oxide-coated product was tested over the pH range of 2–10. Figure 2b indicates a strongly pH-dependent adsorption of HA onto IOCD. The major mechanisms by which NOM adsorbs onto mineral surfaces have been proposed to involve (i) anion exchange (electrostatic interaction), (ii) ligand exchange surface complexation, (iii) hydrophobic interaction, (iv) the entropic effect, (v) hydrogen bonding, and (vi) cation bridging (Gu et al. 1994). Here, a decrease in the adsorption of HA with increasing pH seems consistent with the anion exchange or electrostatic interaction mechanism, because the surface of the iron oxide-coated product becomes more positively charged while HA becomes less negatively charged as pH decreases. On the other hand, at higher solution pH values, besides the electrostatic repulsion, more OH^- anions may compete with negative ions of HA for adsorption sites on the surface, resulting in the reduction of HA adsorption. These results are in agreement with those reported by Peng et al. (2006), who used montmorillonite-Cu(II)/Fe(III) oxide magnetic material as adsorbent for the removal of HA. Their results showed that adsorption is favored at lower pH values. As reported by Baohua et al. (1994), ligand exchange between carboxyl/hydroxyl functional groups of NOM and iron oxide surfaces could be another dominant interaction mechanism, especially under acidic or slightly acidic conditions. Giasuddin et al. (2007) illustrated that adsorption patterns of HA are consistent with the electrostatic interaction mechanism using nanoscale zerovalent iron (NZVI). In their study, they showed maximum adsorption of HA that occurred in the pH range of 3.0–9.0 and decreased sharply at a pH of over 10.0. Their results also showed that NZVI remains attractive to negatively charged HA as long as it has a positive charge on its surface, suggesting the presence of an electrostatic interaction mechanism.

3.3 Effect of HA on As Uptake

3.3.1 Sorption Isotherms

The adsorption isotherms were evaluated with both the Freundlich and Langmuir models. The Langmuir isotherms revealed better fitted (with higher r^2 values) for the adsorption of As on IOCD at various HA concentrations. The measured equilibrium adsorption isotherms of As(III) and As(V) on IOCD in the presence and absence of HA using Langmuir are shown in Fig. 3. The best fitted parameters for the two isotherm models are given in Table 2. The Langmuir isotherm represents a single-layer adsorption model, and thus, the maximum sorption capacity (Q) may give a representation of the available sites on the adsorbent surface. Table 2 clearly shows that the best fitted Q values of As(III) (Q_m= 20 mg/g) and As(V) (Q_m=7 mg/g) in the single-solute system (only As and IOCD) are much higher than their corresponding capacities in the bi-solute system with HA (co-presence of both As and HA). The Q_m values decreased with increasing HA concentration for both As

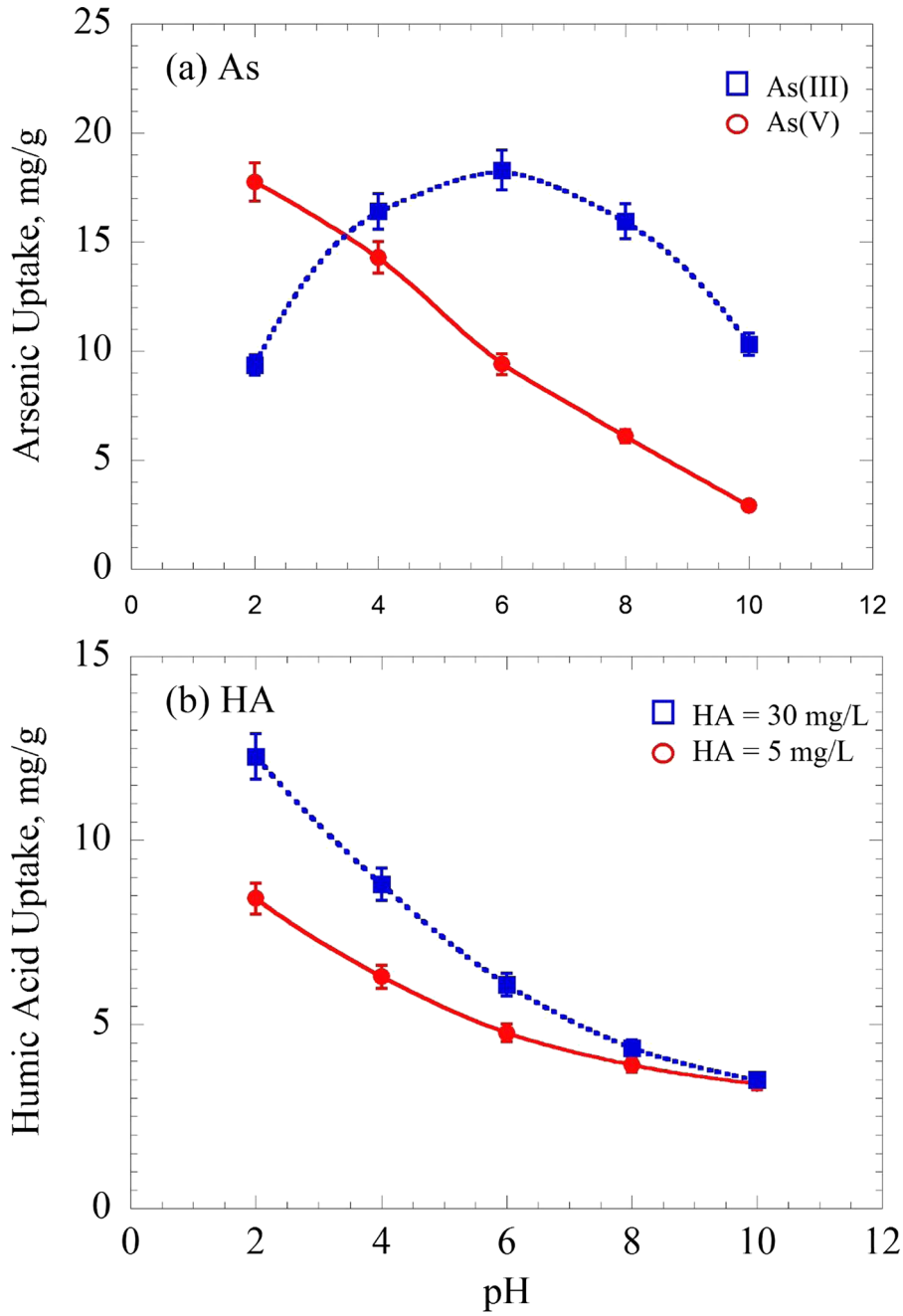

Fig. 2 Effect of pH on uptake of **a** arsenic (with initial concentration=5 mg/L) and **b** humic acid (with initial concentration=5 and 30 mg/L) onto IOCD

species, being only 12.34 and 3.40 mg/g for As(III) and As(V) for HA concentration of 30 mg/L, respectively. This observation may imply that the adsorptions of As(V) and As(III) are both strongly suppressed by the presence of HA. Similar observations were obtained by Giasuddin et al. (2007) where removal of 2 mg/L As(III) and As(V), at 0.3 g/L NZVI, is reduced in the presence of HA (20 mg/L). The reduction was attributed to several factors, including the occupation of a large proportion of sorption sites by HA, slowing the rate of arsenic

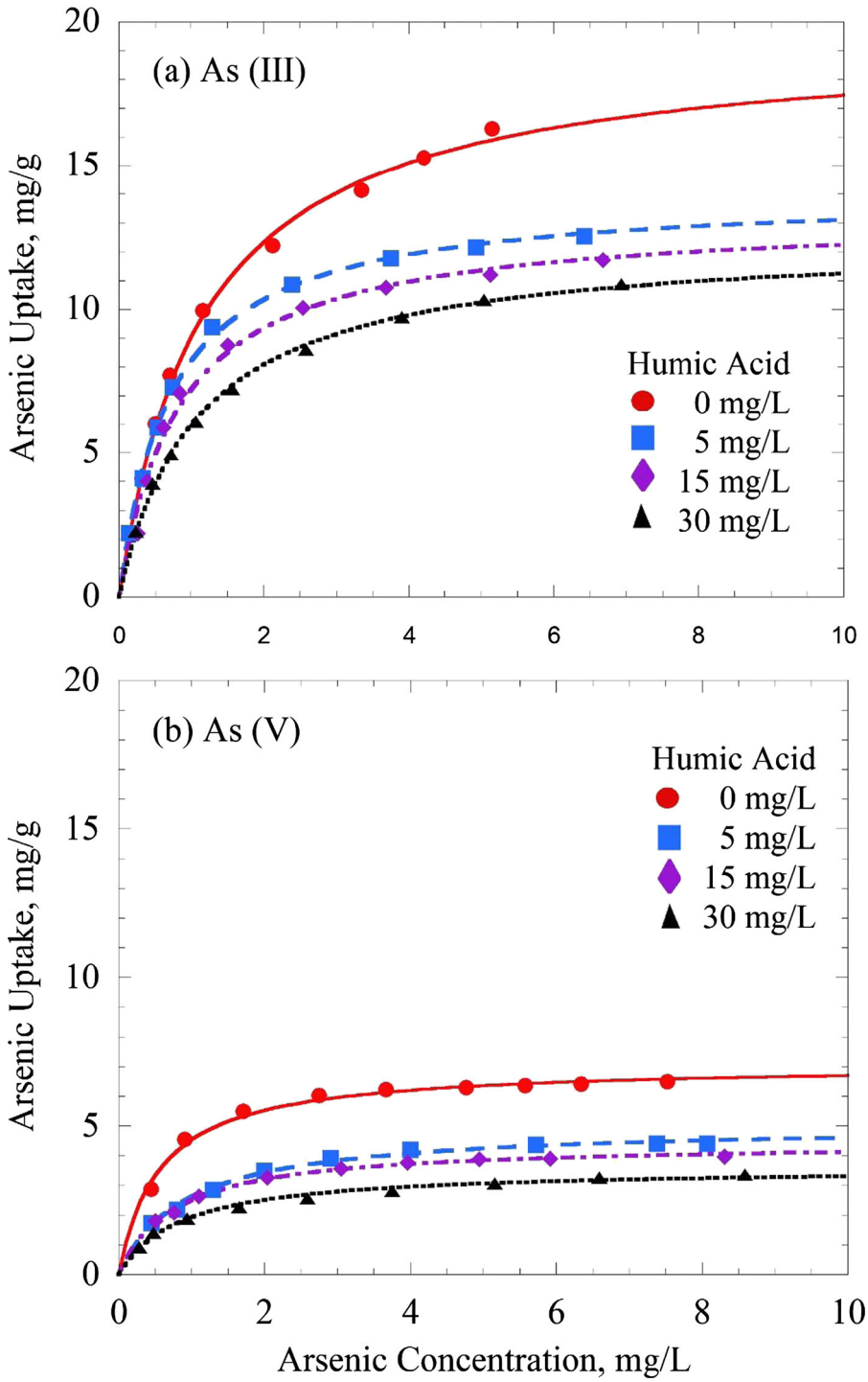

Fig. 3 Impact of humic acid on uptake of **a** As(III) and **b** As(V) onto IOCD at pH=7.5. The curves were fitted with the Langmuir isotherm equations shown in Table 1

species toward favorable sites, and the reduction of corrosion (formation of new sites) rates of NZVI by HA (Redman, et al. 2002; Giasuddin et al. 2007). Luo et al. (2006) also argued that the presence of oxalate/HA retarded the sorption equilibrium, decreasing the observed sorption capacity of As(V) for soil.

Table 2 Parameters of Freundlich and Langmuir models for arsenic sorption to IOCD

Arsenic species	HA conc. (mg/L)	Freundlich			Langmuir		
		K_F ((mg/g)/(mg/L)$^{1/n}$)	$1/n$	r^2	Q_m (mg/g)	Ka (L/mg)	r^2
As(III)	0	8.22	0.48	0.962	20.00	0.83	0.997
	5	6.80	0.43	0.916	14.08	1.39	0.999
	15	6.02	0.44	0.862	13.50	1.08	0.994
	30	4.90	0.48	0.900	12.34	0.82	0.995
As(V)	0	4.20	0.25	0.859	7.00	1.98	0.999
	5	2.36	0.37	0.900	5.02	1.06	0.997
	15	2.34	0.31	0.914	4.38	1.35	0.998
	30	1.71	0.33	0.927	3.40	1.27	0.998

3.3.2 Quantitative Analysis of Chemicals on IOCD Surface

To have a more clear understanding on the effect of HA in the adsorption process, elements on the surface of IOCD were analyzed quantitatively. The elemental composition of IOCD samples after different adsorption reactions was determined by SEM/EDS. Table 3 shows the element composition of the surface of IOCD after treating with 5 mg/L of As(III) or As(V) in the single-solute system or in the bi-solute system with 30 mg/L of HA.

As compositions for the four tested cases are in accordance with those observed for adsorption capacity, with As(III) > As(V) on IOCD surface and that in the single-solute system > that in the bi-solute system. Although no direct link can be made between the As composition obtained from SEM/EDS and that from the adsorption experiment, the data suggest that the coverage of As on the IOCD surface may be influenced by the presence of HA. The coverage of HA on the IOCD surface is also indicated by the carbon and iron compositions. The compositions of carbon were much higher for the system with HA, while those of iron were much lower, both indicating that HA covered a certain portion of the IOCD surface for the two cases with HA. This is in accordance with the observed reduction of adsorption capacity for As in the bi-solute systems.

3.3.3 Dubinin-Radushkevich Isotherm Model

The Dubinin-Radushkevich (D-R) equation is widely used to express the adsorption isotherms in porous media and successfully applied to effectively describe the adsorption type of different sorption systems (Kim et al. 2004; Urbano et al. 2012). The approach was usually applied to distinguish the physical and chemical adsorption of metal ions, with its mean free energy, E per mole of adsorbate (Foo and Hameed 2010). To understand the nature of the mechanism, the equilibrium data were therefore fitted to the D-R isotherm model (Dubinin 1960):

$$q_e = Q_m \exp\left(-K\left[RT\ln\left(1+\frac{1}{C_e}\right)\right]^2\right) = Q_m \exp\left(-K\varepsilon^2\right) \quad (6)$$

where ε (Polanyi potential) $= RT\ln\left(1+\frac{1}{C_e}\right)$, R is the universal gas constant (J mol^{-1} K^{-1}), T is the temperature

Table 3 EDS analysis of IOCD after being treated with arsenic and HA

System	Elemental composition (atomic %)				
	Oxygen	Silica	Iron	Carbon	Arsenic
IOCD adsorbed with As(III)	28.7	6.7	63.0	–	1.7
IOCD adsorbed with As(V)	29.0	6.0	64.1	–	1.0
IOCD adsorbed with As(III) and HA	31.1	4.3	8.5	55.3	0.9
IOCD adsorbed with As(V) and HA	35.8	4.8	10.6	48.4	0.4

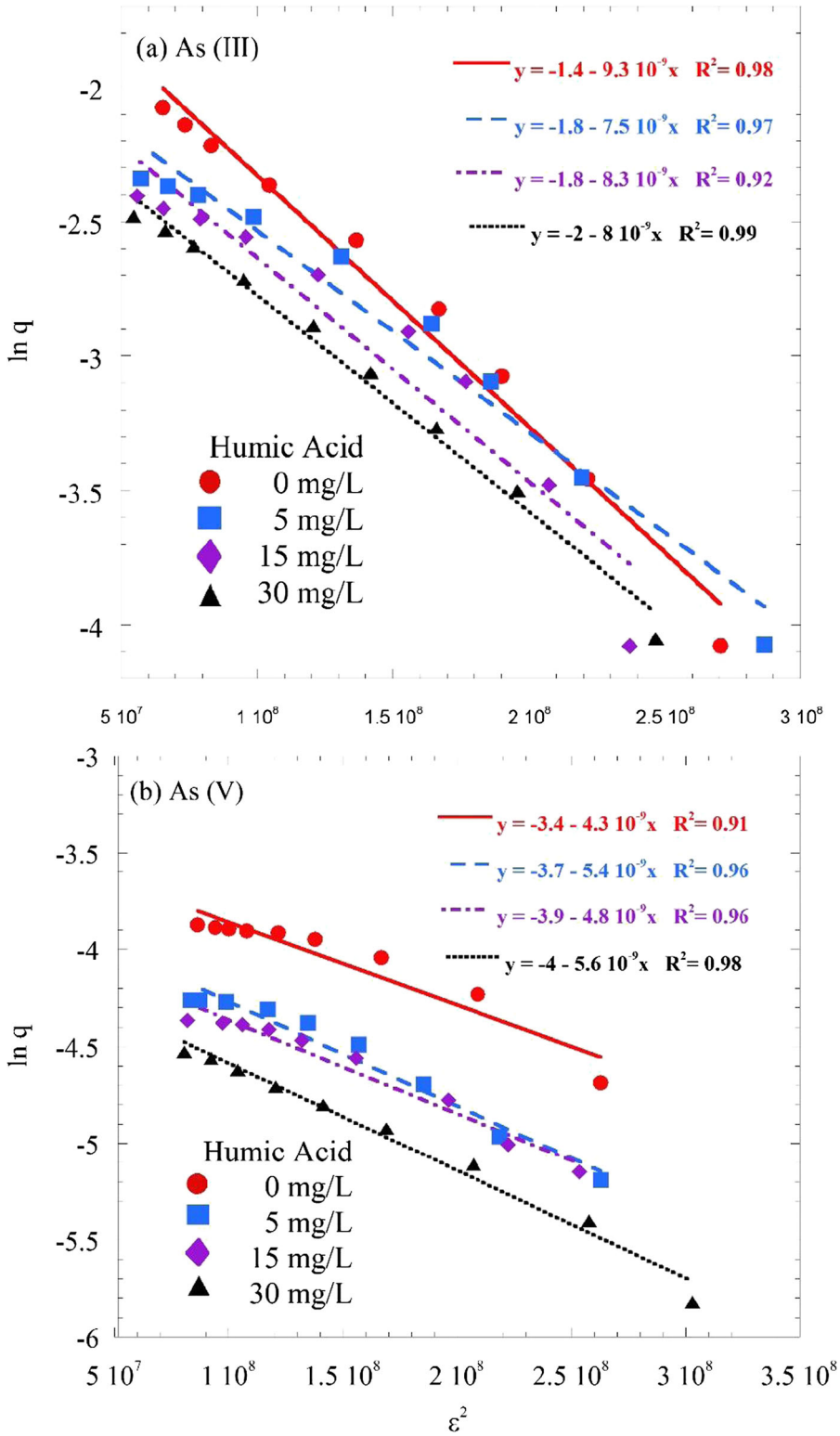

Fig. 4 Sorption data fitted with D-R equations for **a** As(III) and **b** As(V)

(K), q_e is the amount of As sorbed (mmol g^{-1}), C_e is the equilibrium concentration (mmol l^{-1}), Q_m is the D-R constant (mmol g^{-1}), and K (J^{-2} mol^2) is related to the mean free energy of sorption per mole of the sorbate when it is transferred to the surface of the solid from infinity in the solution. The energy of sorption can be further computed using the following relationship (Hasany and Chaudhary 1996):

$$E = \frac{1}{\sqrt{2K}} \tag{7}$$

Figure 4 shows the adsorption data and fitted D-R isotherm models (Eq. (6)) for both As(V) and As(III) onto IOCD under various HA concentrations and at pH=7.5. The figure demonstrates that the sorption data satisfactorily followed the D-R isotherm models, with linear fitted lines and high r^2 values for all the cases, suggesting that the isotherm models reasonably describe the adsorption of As(V) and As(III) onto IOCD in the presence of HA.

Table 4 lists the extracted parameters of the D-R isotherm models, including Q_m, K, and E (as calculated from Eq. (7)). The magnitude of E has been employed to estimate the type of adsorption. If E is in the range of 8–16 kJ mol^{-1}, the interaction between adsorbent and adsorbate can be explained by chemisorption like ion exchange, while for E<8 kJ mol^{-1}, the interaction is considered as physisorption (Bhunia et al. 2007; Chabani et al. 2009). As shown in Table 4, the major interaction between As(III) and IOCD in the single-solute system is closer to physisorption (E= 7.45 kJ mol^{-1}) while that for As(V) is closer to chemisorption (E=11.18 kJ mol^{-1}). This is in accordance with the fact that ion exchange may be present for the As(V)/IOCD system, as at pH=7.5, As(V) is present in anionic form and the surface of IOCD is mainly positively charged. In contrast, at that pH, As(III) is in nonionic form and thus physisorption is expected.

It is also noted that in Table 4, the adsorption energy between As(III) and IOCD increased with increasing HA concentration while that between As(V) and IOCD decreased. These results suggest that as the HA concentration increased, the adsorption system of As(III) moved gradually from physisorption toward the boundary of chemisorption, while the As(V) system moved from chemisorption toward the border of physisorption. Considering the results in Table 3, the presence of HA in the system altered the surface interaction of As species with IOCD indicating that iron oxide surface may be modified by sorbed HA result in changing surface characteristics of the adsorbent and nature of undergoing mechanisms.

3.4 Impact of HA on Adsorption Kinetics

Since the release of As species from bonding sites controls their mobility and bioavailability in the environment, the kinetics of adsorption plays a significant role in controlling their behavior (Bauer and Blodau 2006).

To find the main mechanism in which HA suppresses As uptake, the PDM was employed to simulate the As adsorption kinetics. The PDM combined with the Langmuir model was used to describe the adsorption of As between pore water and the intraparticle pore surface of IOCD. The equilibrium constants for the model input were assumed to be the same as those extracted from the bulk phase equilibrium experiments (Table 2). The pore diffusion coefficient (D_p) was the

Table 4 D-R isotherm parameters for As(III) and As(V)

As species	HA conc. (mg/L)	K (kJ^{-2} mol^2)	(kJ^{-2} mol^1)	r^2	Q_m (mmol g^{-1})
As(III)	0	9.01E-09	7.45	0.980	0.248
	5	8.48E-09	7.68	0.967	0.168
	15	8.39E-09	7.72	0.917	0.164
	30	7.91E-09	7.95	0.948	0.139
As(V)	0	4.00E-09	11.18	0.907	0.032
	5	4.80E-09	10.21	0.946	0.024
	15	5.21E-09	9.8	0.950	0.020
	30	6.01E-09	9.12	0.964	0.017

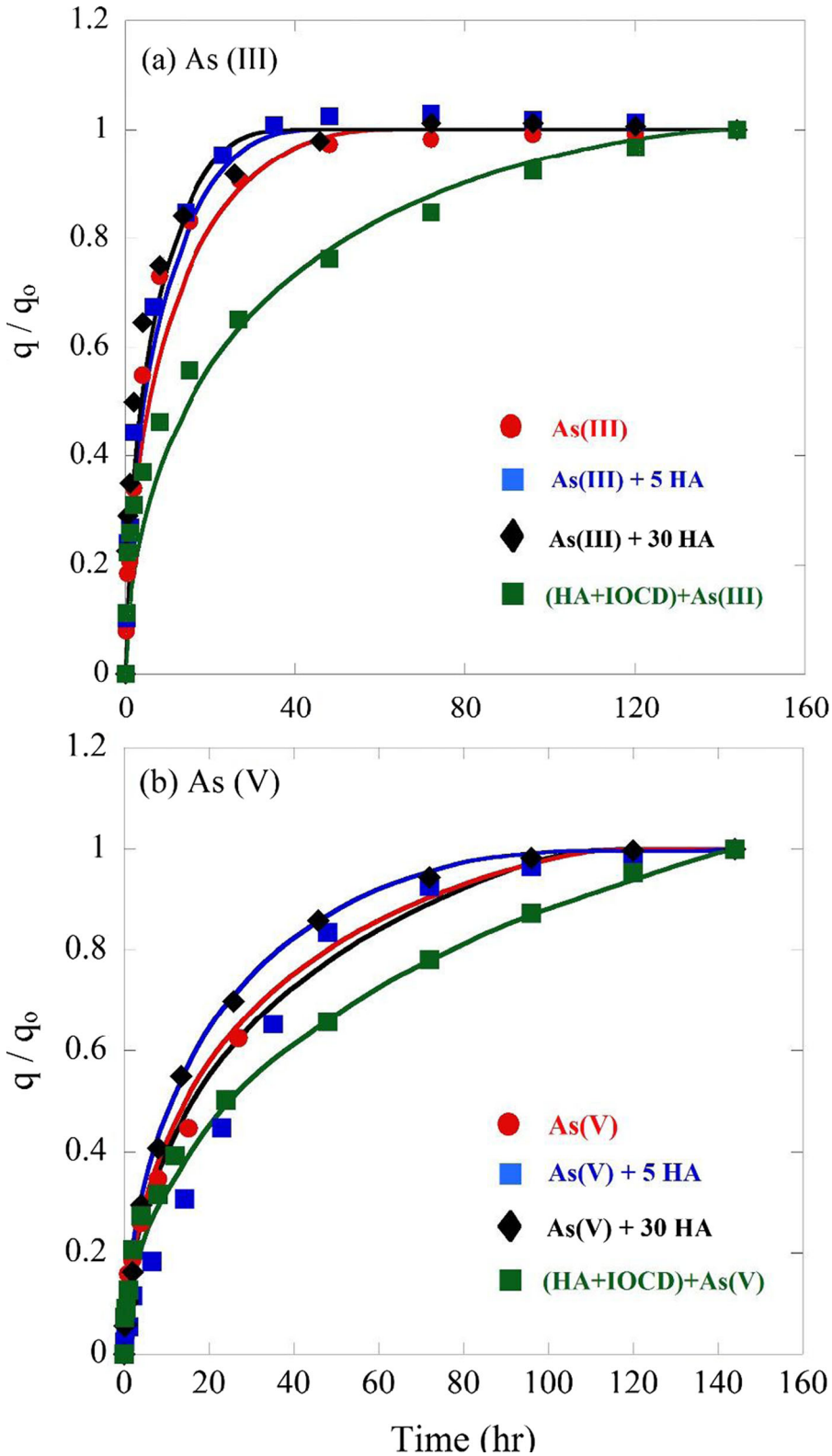

Fig. 5 Experimental data (*symbols*) and fitted pore diffusion model (*lines*) for **a** As(III) and **b** As(V) adsorption onto IOCD-$2_{0.11}$ in the presence and absence of HA (extracted D_p values are listed in Table 4)

only parameter in the model that could be adjusted to fit the experimental data.

All other input properties of IOCD, such as the particle porosity (ε_p, 44.2 %), skeleton density (ρ_p= 2.170 kg/m^3), and grain diameter (d_p=1.7×10^{-4} m), were applied as reported in literature (Lin et al. 1996; Lin 1997; Pan et al. 2010). Tien (1994) indicated that for an adsorption reaction in an agitated system, the interphase mass transfer coefficient (k_f) between the liquid and suspended particles can be linked to the mass transfer coefficient (k_f^*) of the same particles moving at terminal velocity through the same liquid, as developed by Harriott (1962):

$$\frac{k_f}{k_f^*} = 2.0 \tag{8}$$

Harriott (1962) also proposed Eq. (9) to calculate k_f^*. Furthermore, the terminal velocity (u_T) can be estimated using the correlation of Nienow (1969) (Eq. (10)).

$$\frac{k_f^* d_P}{D_M} = 2.0 + 0.6\left[\frac{d_P u_T}{\mu}\right]^{0.5}\left[\frac{\nu}{D_M}\right]^{0.33} \tag{9}$$

$$u_T = \frac{0.153 g^{0.71} d_P^{1.14} \Delta\rho^{0.77}}{\rho^{0.29}\mu^{0.43}} \tag{10}$$

where D_M is the diffusion coefficient of As solute in water (1×10^{-5} cm^2/s), μ is the fluid viscosity (8.01×10^{-3} g s^{-1} cm^{-1}), ν is the kinematic viscosity (8.04×10^{-3} cm^2/s), g is the gravitational acceleration (980 cm/s^2), and $\Delta\rho$ is the density difference between the wet particle density (2.61 g/cm^3) and the liquid density (ρ=0.996 g/cm^3 at 30 °C).

As shown in Fig. 5, the kinetic adsorption data of As species at an initial concentration of 5 mg/L in the presence and absence of HA onto IOCD-2$_{0.11}$ at pH of 7.5 are all well depicted by the PDM combined with the Langmuir isotherm. The extracted pore diffusion coefficients, D_P, for all the tested cases are listed in Table 5. The D_P values are divided in groups for four systems, namely As(III) in IOCD with and without HA, As(III) in HA-preloaded IOCD, As(V) in IOCD with and without HA, and As(V) in HA-preloaded IOCD. For the two systems of As co-sorption with HA in IOCD, where As and HA were simultaneously introduced into the system (systems I and III in Table 5), the D_P values of As are independent of HA concentration, with ~4×10^{-7} and 5×10^{-8} cm^2/s for As(III) and As(V), respectively.

Table 5 Extracted pore diffusion coefficients (D_P) of different systems obtained from PDM* systems I and III: co-sorption of arsenic and HA; systems II and IV: sorption of arsenic onto IOCD pre-sorbed with HA

System*	Experimental condition	Fitted D_p (cm^2/s)
I	As(III) As(III)+5 mg/L HA As(III)+30 mg/L HA	4×10^{-7}
II	(HA+IOCD)+As(III)	7.5×10^{-8}
III	As(V) As(V)+5 mg/L HA As(V)+30 mg/L HA	5×10^{-8}
IV	(HA+IOCD)+As(V)	1×10^{-8}

Unlike in the previous section, which showed that HA may alter the equilibrium of As on IOCD, the kinetic results suggest that HA did not influence the diffusional transport of As in the two systems with As and HA co-sorption. As HA molecules are much bigger than As (Shinozuka et al. 2004), the diffusion coefficient of HA molecules is expected to be smaller. Therefore, diffusional transport of As in the intraparticular pores is expected to be faster and not affected by the presence of HA. It is also interesting to see that the diffusion coefficient of As(V) is smaller than that of As(III). Although the reason for the difference is not clear, one possibility is due to charge difference. As(III) is known to be neutral in the pH range tested, whereas As(V) is negatively charged. As the surface of IOCD is mostly positively charged, the transport of As(V) may be retarded by charge interaction.

Table 5 also shows that for the two systems with HA-preloaded IOCD (systems II and IV), the diffusion coefficients of As are only about 1/5 those in the corresponding systems with no HA preloaded. As identified by SEM/EDS analysis in the previous section (Table 3), HA may accumulate on the surface of IOCD. It is also expected that HA may block the surface, if enough time is given to the intraparticular pores of IOCD. In the aforementioned two systems, IOCD was first pre-sorbed with 30 mg/L of HA. Therefore, for systems II and IV, blockage of certain transport pathways in IOCD is expected, leading to smaller pore diffusion coefficients and longer time for equilibrium for As. This is confirmed by the similar equilibrium capacities of As onto IOCD under the conditions of co-sorption with HA and preloaded with HA. Experimental results of both As species show that the As adsorption capacity is not

affected by the time of HA loading, suggesting that the pores were not completely blocked. The partial pore blockage only slows down the transport, and since there is no complete blockage of the pores, the equilibrium capacity is not affected.

4 Conclusion

The presence of HA was shown to affect the sorption of As onto the tested iron oxide-based adsorbent, IOCD. The uptakes of both As(V) and As(III) onto IOCD were suppressed by HA in the solution, with the impact increasing with increasing HA concentration. As suggested by the results from the surface analysis of IOCD using SEM/EDS, the suppression of As uptake may be attributed to a portion of sorption sites being covered by HA. Adsorption energy calculated based on the D-R isotherm model indicates that the major interaction between As(III) and IOCD in the single-solute system is due to physisorption while that for As(V) is closer to chemisorption. However, when HA was present in the systems, the adsorption energies of As(III) and As(V) onto IOCD increased and decreased with increasing HA concentration, respectively. The results suggest that the presence of HA in the system may alter the surface interaction of As species with IOCD, with As(III) moving from physisorption toward chemisorptions and As(V) moving from chemisorption toward physisorption. Kinetic results reveal that the diffusional transport of As onto IOCD was not affected by the presence of HA in the solution, probably due to the fact that the diffusion of HA molecules is slower than that of As. However, when sorbed onto HA-preloaded IOCD, the diffusion coefficients of both As species were only 1/5 those in the corresponding systems with no HA preloaded. The slow processes for reaching equilibrium may be attributed to pore blockage by the preloaded HA in IOCD. Therefore, for an iron oxide-based porous adsorbent, the presence of HA or NOM may reduce the adsorption uptake due to site coverage and slow down of the transport process due to partial pore blockage. The results demonstrate that HA has competitive effects with As resulting in control the mobility of As in the environment, and these effects should be taken into account during the application of iron oxide-based adsorbents for treatment and remediation of As-contaminated groundwater.

Acknowledgments This research is supported by Taiwan National Science Council under Grant Number NSC 100-2221-E-006-036-MY3.

References

Anawar, H. M., Akai, J., Komaki, K., Hiroshi, T., Takahito, Y., Toshio, I., Syed, S., & Kikuo, K. (2003). Geochemical occurrence of arsenic in groundwater of Bangladesh: source and mobilization processes. *Journal of Geochemical Exploration, 77*, 109–131.

Bahar, M. M., Megharaj, M., & Naidu, R. (2013). Bioremediation of As-contaminated water: recent advances and future prospects. *Water, Air, and Soil Pollution, 224*, 1722.

Baohua, G. U., Schmitt, J., Chen, Z., Liang, L., & McCarthy, J. F. (1994). Adsorption and desorption of natural organic matter on iron oxide: mechanisms and models. *Environmental Science and Technology, 28*(1), 38–46.

Bard, A. J., Parsons, R., & Jordan, J. (1985). *Standard potentials in aqueous solution*. New York: Dekker.

Bauer, M., & Blodau, C. (2006). Mobilization of As by dissolved organic matter from iron oxides, soils and sediments. *Science of the Total Environment, 354*, 179–190.

Benjamin, M. M., Sletten, R. S., Bailey, R. P., & Bennet, T. (1996). Sorption and filtration of metals using iron-oxide-coated sand. *Water Research, 30*(11), 2609–2619.

Bhunia, P., Pal, P., & Bandyopadhyay, M. (2007). Assessing As leachability from pulverized cement concrete produced from As-laden solid CalSiCo-sludge. *Journal Hazardous Material, 141*(3), 826–833.

Biswas, B.K., & Loeppert, R.H. (2003). Adsorption of As(V)/As(III) on TiO2 and the photocatalytic oxidation of As(III). *7th International Conference on the Biogeochemistry of Trace Elements*, Uppsala, Sweden

Chabani, M., Amrane, A., & Bensmaili, A. (2009). Equilibrium sorption isotherms for nitrate on resin Amberlite IRA 400. *J Hazard Mat, 165*, 27–33.

Cullen, W. R., & Reimer, K. J. (1989). Arsenic speciation in the environment. *Chemical Reviews, 89*, 713–764.

Deschamps, E., Ciminelli, V., Weidler, P. G., & Ramos, A. Y. (2003). As sorption onto soils enriched in Mn and Fe minerals. *Clays and Clay Minerals, 51*, 197–204.

Dhiman, A. K., & Chaudhuri, M. (2007). Iron and manganese amended activated alumina—a medium for adsorption/oxidation of arsenic from water. *Journal of Water Supply: Research and Technology - AQUA, 56*, 69–74.

Dixit, S., & Hering, J. G. (2003). Comparison of arsenic (V) and arsenic (III) sorption onto iron oxide minerals: implications for arsenic mobility. *Environmental Science and Technology, 37*, 4182–4189.

Dubinin, M. M. (1960). The potential theory of adsorption of gases and vapors for adsorbents with energetically non-uniform surface. *Chemical Reviews, 60*, 235–266.

Eaton, A. (1995). Measuring UV-absorbing organics: a standard method. *Journal AWWA, 87*, 86–90.

Ferguson, J.F., & Anderson, M.A. (1974). Chemical forms of As in water supplies and their removal. In: Chemistry of water

supply, treatment, and distribution; Rubin, A. J., Ed.; Ann Arbor Science, Ann Arbor, MI, 1974; pp 137–158.

Foo, K. Y., & Hameed, B. H. (2010). Insights into the modeling of adsorption isotherm systems. *Chemical Engineering Journal, 156*, 2–10.

Fox, L. E. (1983). The removal of dissolved humic acid during estuarine mixing. *Estuarine, Coastal and Shelf Science, 16*, 431–440.

Freundlich, H. M. F. (1906). Über die Adsorption in Lösungen. *Zeitschrift für Physikalische Chemie-Leipzig, 57A*, 385–470.

Giasuddin, A. B. M., Kanel, S. R., & Choi, H. (2007). Adsorption of humic acid onto nano scale zerovalent iron and its effect on As removal. *Environmental Science and Technology, 41*, 2022–2027.

Gu, B., Schmitt, J., Chen, Z., Liang, L., & McCarthy, J. F. (1994). Adsorption and desorption of natural organic matter on iron oxide: mechanisms and models. *Environmental Science and Technology, 28*, 38–46.

Guan, X., Dong, H., Ma, J., & Jiang, L. (2009). Removal of As from water: effects of competing anions on As(III) removal in KMnO4–Fe(II) process. *Water Research, 43*, 3891–3899.

Guo, H., Zhong, Z., Lei, M., Xue, X., Wan, X., Zhao, J., & Chen, T. (2012). As uptake from As-contaminated water using hyperaccumulator Pteris vittata L.: effect of chloride, bicarbonate, and As species. *Water, Air, and Soil Pollution, 223*, 4209–4220.

Harriott, P. (1962). Mass transfer to particles: part I. Suspended in agitated tanks. *AIChE Journal, 8*, 93–101.

Hasany, S. M., & Chaudhary, M. H. (1996). Sorption potential of Hare River sand for the removal of antimony from acidic aqueous solution. *Applied Radiation and Isotopes, 47*, 467–471.

Ho, Y. S., Huang, C. T., & Huang, H. W. (2002). Equilibrium sorption isotherm for metal ions on tree fern. *Process Biochemistry, 37*, 1421–1430.

Hristovski, K. D., Westerhoff, P. K., Möllerc, T., & Sylvester, P. (2009). Effect of synthesis conditions on nano-iron (hydr)oxide impregnated granulated activated carbon. *Chemical Engineering Journal, 146*, 237–243.

Jang, M., Chen, W., & Cannon, F. S. (2008). Preloading hydrous ferric oxide into granular activated carbon for arsenic removal. *Environmental Science and Technology, 42*, 3369–3374.

Jansen, S. A., Malaty, M., Nwabara, S., Johnson, E., Ghabbour, E., Davies, G., & Varnum, J. M. (1996). Structural modeling in humic acids. *Materials Science and Engineering C, 4*, 175–179.

Jeon, C. S., Baek, K., Park, J. K., Oh, Y. K., & Lee, S. D. (2009). Adsorption characteristics of AsV on iron-coated zeolite. *Journal of Hazardous Materials, 163*, 804–808.

Jiménez-Cedillo, M. J., Olguín, M. T., & Fall, C. (2009). Adsorption kinetic of arsenates as water pollutant on iron, manganese and iron-manganese-modified clinoptilolite-rich tuffs. *Journal of Hazardous Materials, 163*, 939–945.

Kalbitz, K., & Wennrich, R. (1998). Mobilization of heavy metals and arsenic in polluted wetland soils and its dependence on dissolved organic matter. *Science of the Total Environment, 209*, 27–39.

Kim, Y., Kim, C., Choi, I., Rengaraj, S., & YI, A. (2004). As removal using mesoporous alumina prepared via a templating method. *Environmental Science and Technology, 38*, 924–931.

Kundu, S., & Gupta, A. K. (2006). Arsenic adsorption onto iron oxide coated cement (IOCC): regression analysis of equilibrium data with several isotherm models and their optimization. *Chemical Engineering Journal, 122*, 93–106.

Lai, C. H., Lo, S. L., & Chiang, H. L. (2000). Adsorption/desorption properties of copper ions on the surface of iron-coated sand using BET and EDAX analysis. *Chemosphere, 41*, 1249–1255.

Langmuir, I. (1918). The adsorption of gases on plane surfaces of glass, mica and platinum. *Journal of the American Chemical Society, 40*, 1361–1403.

Lin, T. F. (1997). Diffusion and sorption of water vapor and benzene within a dry model soil organic matter. *Water Science and Technology, 35*, 131–138.

Lin, T. F., & Wu, J. K. (2001). Adsorption of arsenite and arsenate within activated alumina grains: equilibrium and kinetics. *Water Research, 35*, 2049–2057.

Lin, T. F., Little, J. C., & Nazaroff, W. W. (1996). Transport and sorption of organic gases in activated carbon. *Journal of Environmental Engineering, 122*, 169–175.

Lin, T. F., Hsiao, H. C., Wu, J. K., Hsiao, H. C., & Yeh, J.-H. (2002). Removal of arsenic from groundwater using point-of-use reverse osmosis and distilling devices. *Environmental Technology, 23*, 781–79.

Lin, T. F., Liu, C. C., & Hsieh, W. H. (2006). Adsorption kinetics and equilibrium of arsenic onto an iron-based adsorbent and an ion exchange resin. *Water Supply, 6*(2), 201–207.

Liu, C., Wang, X., Li, X., Cao, W., & Yang, J. (2012). Detoxification of arsenite through adsorption and oxidative transformation on pyrolusite. *Clean – Soil, Air, Water, 0*, 1–8.

Liu, F., Fan, J., Wanga, S., & Mab, G. (2013). Adsorption of natural organic matter analogues by multi-walled carbon nanotubes: comparison with powdered activated carbon. *Chemical Engineering Journal, 219*, 450–458.

Loffredo, L., & Senesi, N. (2006). The role of humic substances in the fate of anthropogenic organic pollutants in soil with emphasis on endocrine disruptor compounds. I. Twardowska et al. (eds.), *Soil and Water Pollution Monitoring, Protection and Remediation*, 3–23.

Luo, L., Zhang, S., Shan, X. Q., & Zhu, Y. G. (2006). Effects of oxalate and humic acid on arsenate sorption by and desorption from a Chinese red soil. *Water, Air, and Soil Pollution, 176*, 269–283.

Lv, X., Hu, Y., Tang, J., Sheng, T., Jiang, G., & Xu, X. (2013). Effects of co-existing ions and natural organic matter on removal of chromium (VI) from aqueous solution by nanoscale zero valent iron (nZVI)-Fe3O4 nanocomposites. *Chemical Engineering Journal, 218*, 55–64.

Mandal, B. K., & Suzuki, K. T. (2002). Arsenic round the world: a review. *Talanta, 58*, 201–235.

Manna, B. R., Dey, S., Debnath, S., & Ghosh, U. C. (2003). Removal of As from groundwater using crystalline hydrous ferric oxide (CHFO). *Water Quality Research Journal of Canada, 38*(1), 193–210.

Markovski, J. S., Markovic, D. D., Dokic, V. R., Mitric, M., Ristic, M. D., Onjia, A. E., & Marinkovic, A. D. (2014). Arsenate adsorption on waste eggshell modified by goethite, α-MnO2 and goethite/α-MnO2. *Chemical Engineering Journal, 237*, 430–442.

Matschullat, J. (2000). Arsenic in the geosphere—a review. *Science of the Total Environment, 249*, 297–312.

Mondal, P., Majumder, C. B., & Mohanty, B. (2007). A laboratory study for the treatment of arsenic, iron, and manganese bearing ground water using Fe+3 impregnated activated carbon: effects of shaking time, pH and temperature. *Journal of Hazardous Materials, 144*(1–2), 420–426.

Murphy, E. M., Zachara, J. M., Smith, S. C., & Phillips, J. L. (1992). The sorption of humic acids to mineral surfaces and their role in contaminant binding. *Science of the Total Environment, 117/118*, 413–423.

Najm, I. N., Patania, N. L., Jacangelo, J. G., & Krasner, S. W. (1994). Evaluating surrogates for disinfection by-products (DBPs). *Journal AWWA, 86*(6), 98–106.

Nayak, B., Amir Hossain, M. D., Sengupta, M. K., Ahamed, S., Das, B., Pal, A., & Mukherjee, A. (2006). Adsorption studies with arsenic onto ferric hydroxide gel in a non-oxidizing environment: the effect of co-occurring solutes and speciation. *Water Quality Research Journal Of Canada, 41*(3), 333–340.

Nienow, A. W. (1969). Dissolution mass transfer in a turbine agitated baffled vessel. *Canadian Journal of Chemical Engineering, 4*, 248–258.

Pan, Y. F., Chiou, C. T., & Lin, T. F. (2010). Adsorption of As(V) by iron-oxide-coated diatomite (IOCD). *Environmental Science and Pollution Research, 17*, 1401–1410.

Peng, X., Luan, Z., & Zhang, H. (2006). Montmorillonite Cu(II)/Fe(III) oxides magnetic material as adsorbent for removal of humic acid and its thermal regeneration. *Chemosphere, 63*, 300–306.

Pierce, M. L., & Moore, C. B. (1982). Adsorption of arsenite and arsenate on amorphous iron hydroxide. *Water Research, 16*, 1247–1253.

Ramesh, A., Hasegawa, H., Maki, T., & Ueda, K. (2007). Adsorption of inorganic and organic arsenic from aqueous solutions by polymeric Al/Fe modified montmorillonite. *Separation and Purification Technology, 56*(1), 90–100.

Raven, K. P., Jain, A., & Loeppert, R. H. (1998). Arsenite and arsenate adsorption on ferrihydrite: kinetics, equilibrium, and adsorption envelopes. *Environmental Science and Technology, 32*, 344–349.

Redman, A. D., Macalady, D. L., & Ahmann, D. (2002). Natural organic matter affects As speciation and sorption onto hematite. *Environmental Science and Technology, 36*, 2889–2896.

Rodrigues, A., Brito, A., Janknecht, P., Proenc, M. F., & Nogueira, R. (2008). Quantification of humic acids in surface water: effects of divalent cations, pH, and filtration. *Journal of Environmental Monitoring, 11*, 377–382.

Shinozuka, T., Shibata, M., & Yamaguchi, T. (2004). Molecular weight characterization of humic substances by MALDI-TOF-MS. *Journal of Mass Spectrometry Society of Japan, 52*(1), 29–32.

Simsek, E. S., Özdemir, E., & Beker, U. (2013). Process optimization for As adsorption onto natural zeolite incorporating metal oxides by response surface methodology. *Water, Air, and Soil Pollution, 224*, 1614.

Singh, D. B., Prasad, G., Rupainwar, D. C., & Singh, V. N. (1988). As(III) removal from aqueous solution by adsorption. *Water, Air, and Soil Pollution, 42*, 373–386.

Smedley, P. L., & Kinniburgh, D. G. (2002). A review of the source, behaviour and distribution of arsenic in natural waters. *Applied Geochemistry, 17*, 517–568.

Summers, R. S., Haist, B., Koehler, J., Ritz, J., Zimmers, G., & Sontheimer, H. (1989). The influence of background organic matter on GAC adsorption. *Journal of American Water Works Association, 81*(5), 66–72.

Sun, X., & Doner, H. E. (1998). Adsorption and oxidation of arsenite on goethite. *Soil Science, 163*, 278–287.

Tamaki, S., & Frankenberger, W. T. (1992). Environmental biochemistry of arsenic. *Reviews of Environmental Contamination and Toxicology, 124*, 79–110.

Tien. C. (1994). Adsorption calculation and modeling. Butterworth-Heinemann, MA.

TWEPA. (2014). *National drinking water quality standards*. Taipei, Taiwan: TWEPA.

Urbano, B. F., Rivas, B. L., Martinez, F., & Alexandratos, S. D. (2012). Equilibrium and kinetic study of As sorption by water-insoluble nanocomposite resin of poly[N-(4-vinylbenzyl)-N-methyl-D-glucamine]- montmorillonite. *Chemical Engineering Journal, 93*(194), 21–30.

USEPA, (1999). Technologies and costs for removal of As from drinking water. EPA 815: P-01-001.

USEPA. (2001). National primary drinking water regulations: As and clarifications to compliance and new source contaminants monitoring. *Federal Register, 14*, 6975–7066.

Wilkie, J. A., & Hering, J. G. (1996). Adsorption of arsenic onto ferric hydroxide: effects of adsorbate/adsorbent ratios and co-occurring solutes. *Colloids Surface A, 107*, 97–110.

Yoshida, T., Yamauchi, H., & Sun, G. F. (2004). Chronic health effects in people exposed to As via the drinking water: dose–response relationships in review. *Toxicology and Applied Pharmacology, 198*, 243–252.

Yu, X. (2001). Humic acids from endemic arsenicosis areas in inner Mongolia and from the blackfoot diseaseareas in Taiwan: a comparative study. *Environmental Geochemistry and Health, 23*, 27–42.

Yuan, J. R., Ghosh, M. M., & Teoh, R. S. (1987). Adsorption of As on hydrous oxides. In: Kolaczkowski S.T.,Crittenden B.D., editors. *Management of Hazardous and Toxic Wastes in the Process Industries* (pp. 363–371). London, UK: Elsevier Applied Science

Zeng, L. (2004). Arsenic adsorption from aqueous solutions on an Fe(III)-Si binary oxide adsorbent. *Water Quality Research Journal, 39*(3), 267–275.

Zhou, W., Fu, H., Pan, K., Tian, C., Qu, Y., Lu, P., & Sun, C. C. (2008). Mesoporous TiO2/α-Fe_2O_3: bifunctional composites for effective elimination of arsenite contamination through simultaneous photocatalytic oxidation and adsorption. *The Journal of Physical Chemistry C, 112*, 19584–19589.